



City Research Online

City, University of London Institutional Repository

Citation: Papadopoulos, Konstantinos, Gavaises, M. and Atkin, C. (2014). A simplified mathematical model for thrombin generation. Medical Engineering and Physics, 36(2), pp. 196-204. doi: 10.1016/j.medengphy.2013.10.012

This is the accepted version of the paper.

This version of the publication may differ from the final published version.

Permanent repository link: <https://openaccess.city.ac.uk/id/eprint/13568/>

Link to published version: <http://dx.doi.org/10.1016/j.medengphy.2013.10.012>

Copyright: City Research Online aims to make research outputs of City, University of London available to a wider audience. Copyright and Moral Rights remain with the author(s) and/or copyright holders. URLs from City Research Online may be freely distributed and linked to.

Reuse: Copies of full items can be used for personal research or study, educational, or not-for-profit purposes without prior permission or charge. Provided that the authors, title and full bibliographic details are credited, a hyperlink and/or URL is given for the original metadata page and the content is not changed in any way.

A simplified mathematical model for thrombin generation

Papadopoulos Kostis, Gavaises Manolis and Chris Atkin
School of Engineering and Mathematical Sciences

City University London

Northampton square, London

EC1V 0HB

Room: C171

Phone: +44 (0) 20 7040 8115

Fax: +44 (0) 20 7040 8566

Email: Papadopoulos.Konstantinos.1@city.ac.uk :
M.Gavaises@city.ac.uk

Abstract

A new phenomenological mathematical model based directly on laboratory data for thrombin generation and having a patient-specific character is described. A set of the solved equations for cell-based models of blood coagulation that can reproduce the temporal evolution of thrombin generation is proposed; such equations are appropriate for use in Computational Fluid Dynamics (CFD) simulations. The initial values for the reaction rates are either taken from already existing model or experimental data, or they can be obtained from simple reasoning under certain assumptions; it is shown that coefficients can be adjusted in order to fit a range of different thrombin generation curves as derived from thrombin generation assays. The behaviour of the model for different platelet concentration seems to be in good agreement with reported experimental data. It is shown that the reduced set of equations used represents to a good approximation a low-order model of the detailed mechanism and thus it can represent a cost-effective and-case specific mathematical model of coagulation reactions up to thrombin generation

Keywords:

CFD, coagulation, simulation, thrombus

Introduction

The formation of thrombus in blood is involved in a number of life threatening situations like Coronary Artery Disease and mechanical heart valve complications; it is a multi-scale phenomenon both in respect of time and space, involving a number of biochemical substances, blood circulating minerals and cellular responses. While the formation of blood clot is a physiological response of human body to vessel injury, it can be initiated when blood

contacts certain substances like those exposed after the rupture of atheromatous plaques in stenosed vessels [Rauch, Osende et al. 2001] and when pathological flow conditions prevail in a region [Nesbitt, Westein et al. 2009]. Between the initiation and the formation of a thrombus, a series of enzymatic reactions takes place also known as coagulation cascade [Furie and Furie 2008], classically divided in three parts: (1) the extrinsic or Tissue Factor (TF) pathway, (2) the intrinsic or contact pathway and the (3) common pathway. In every step of the process a circulating zymogen is activated, with the activation reaction being catalysed by the products of previous steps. However, as most of these enzymatic reactions take place on cell membranes, the current approaches for coagulation are cell-based models and the process is divided in three discrete phases, initiation, amplification and propagation. Thrombin (factor IIa) and platelets play critical roles in the coagulation process. Thrombin in the final step catalyses the conversion of fibrinogen (factor I) to fibrin (factor Ia), a protein that through polymerization creates a mesh clot that also traps circulating blood cells. In addition, thrombin activates factor XIII (that forms bonds that crosslink the fibrin strands [Mosesson 2005]), causes the activation of platelets [Brass 2003], the activation of factors V and VIII and their inhibitor protein C (APC). Platelets on the other hand, after activation by chemical or mechanical stimulation [Jesty, Yin et al. 2003] become adhesive and form aggregates on the materials exposed after arterial damage [Badimon, Badimon et al. 1986] or plaque rupture [Fernández-Ortiz, Badimon et al. 1994; Reininger, Bernlochner et al. 2010] or in flowing blood. In addition they play a major role in thrombin formation [Rosing, van Rijn et al. 1985; Monroe, Hoffman et al. 2002] and they enhance the coagulation process by supporting on their membrane some of the coagulation reactions [Smith 2009], releasing chemical substances and micro-particles [Rendu and Brohard-Bohn 2001] that influence the progress of coagulation and activate other platelets.

The advance of computational techniques and increase of computational power have made

possible the emergence of in silico studies that reproduce a part of or the whole process in greater or lesser detail, simulating either the whole process of thrombus formation or only the coagulation reaction system up to thrombin or fibrin production. The first mathematical simulation of thrombin and fibrin generation in plasma used exponential time functions as fixed inputs for concentration of some enzymes [Willems, Lindhout et al. 1991]. In vitro measurements of the reaction rate constants [Lawson, Kalafatis et al. 1994] were used for the development of a system of 20 reactions, including formation and breakage of complexes, in a study that mainly focused on the effect of variation of the concentration of different factors [Jones and Mann 1994]. A similar model was proposed for the intrinsic pathway including fibrin production and APC inhibition mechanism, and was used to investigate threshold values for some enzymes and the spatial propagation of coagulation from the reacting site due to diffusion [Zarnitsina, Pokhilko et al. 1996; Zarnitsina, Pokhilko et al. 1996]. Subsequent work included more chemical substances and biochemical processes [Hockin, Jones et al. 2002] up to thrombin production, resulting in a system consisting of 27 reactions and 42 reaction rate constants that later was combined with a Monte Carlo simulation method, in order to detect changes to the cascade initiation behaviour, due to small variation of the concentration of enzymes induced by the stochastic approach [Lo, Denney et al. 2005]. At the same time some studies used simulations to investigate a specific part of the coagulation cascade, as the function of positive feedback loops and threshold concentrations for cascade initiation [Beltrami and Jesty 1995], the triggering threshold with respect to Tissue Factor Pathway Inhibitor (TFPI) [Xu, Hu Xu et al. 2005] or the inhibition mechanism of APC [Qiao, Xu et al. 2004].

The studies that simulate thrombus formation and growth, simultaneously with blood flow and concentration of related substances, necessitate a less detailed sub-model for the coagulation cascade. While for the first studies of this kind the production rates of substances

76 were mainly modelled as fluxes or with the use of few reactions [Hubbell and McIntire 1986;
77 Folie and McIntire 1989], the increase of computational power allowed more complicated
78 multi-scale and multi-phase models to emerge, that include an integrated coagulation sub-
79 model. The authors of [Kuharsky and Fogelson 2001] proposed an integrated model of
80 thrombus formation under flow conditions, taking into account the localization of reactions
81 on surfaces, with the inclusion of the available binding sites on cell membranes for enzymes
82 and using a system of 59 equations to simulate the coagulation system up to thrombin
83 generation. A study that modelled platelet-platelet and platelet-wall interaction as reversible
84 elastic links demonstrated the influence of these interactions on the flow field and predicted
85 thrombus evolution and emboli formation [Fogelson and Guy 2004]. The initial model was
86 later improved with the addition of the APC mechanism and the transport of substances
87 between plasma and endothelium cells [Fogelson and Tania 2005]. The same concepts for
88 cells and reactions were combined with an immersed boundary method [Lai and Peskin 2000;
89 Peskin 2002] for modelling platelet movement and the interaction between platelet membrane
90 sites and chemicals or endothelium. The results of this micro-scale model were also used to
91 develop a continuous model for platelet aggregation (with platelets as continuous phase with
92 movement limitations) describing the alterations in blood flow due to the presence of
93 aggregated platelets [Fogelson and Guy 2008]. The macro-scale model was tested in
94 simulations with pulsating flow in an idealized two dimensional vessel bifurcation [Yang,
95 Lewis et al. 2004]. The continuous model, with coupling of flow with thrombus growth and
96 including flow and transport within the thrombus, was used to demonstrate the effects of flow
97 conditions and the quantity of TF exposed in thrombus growth [Leiderman and Fogelson
98 2011]. Anand et al [Anand, Rajagopal et al. 2003; Anand, Rajagopal et al. 2005] presented
99 another multi-process model that used a viscoelastic model to simulate flow for both free
100 vessel lumen and clot. This model also incorporated the activation of platelets due to

excessive shear stress and fibrin production and lysis. In a similar work, a model for the viscosity of blood depending on fibrin concentration was proposed and used in a three-dimensional simulation of blood coagulation in a tube with a reacting site; in this study the area where fibrin concentration exceeded a specific value interpreted as the area occupied by the clot[Bodnár and Sequeira 2008]. In [Xu, Chen et al. 2008] another multi-scale model was proposed that included a cellular pot model [Marée, Grieneisen et al. 2007] for discrete cells and cell movement was simulated through an energy-based stochastic process. The simulation involved differentiation of cell movements depending on fibrin levels and cell-cell or cell-surface interaction and bonds. The model was used to evaluate the role of fVII in venous thrombus formation due to vessel injury [Xu, Lioi et al. 2010] and to examine the impact of pulsating flow and the non-Newtonian characteristics of blood on thrombus growth [Xu, Chen et al. 2009].

While the detailed description of coagulation included in these works makes them appropriate for studying the influence of different factors, unfortunately it increases dramatically the computational cost; thus published applications mainly refer to small two dimensional regions ($\sim 100\mu\text{m}$) while the dimensions of computational regions for studying thrombus formation in a coronary artery or in mechanical heart valves are much larger (typically, the diameter of the coronary artery is about 4mm while the diameter of the aortic root is of some cm) with the flow distribution being three-dimensional and strongly time dependent preventing use of simplified flow models. In addition, these models do not have patient-specific characteristics, as the use of reaction rate constants derived from experiments do not allow the significant variability of thrombin generation observed for different individuals [Oliver, Monroe et al. 1999]. At the same time, it has been shown that the resulting thrombin generation curve predicted by such models under steady state conditions can be simulated in different ways by a much simpler system of 6 equations [Wagenvoort, Hemker et al. 2006].

As the process between the initial stimulation and the formation of thrombin consist the main part of the coagulation reactions, our motivation is to develop a phenomenological model for thrombin formation that would be efficient enough to be used with three dimensional Computational Fluid Dynamic (CFD) simulations while also being adjustable in order to reflect measured differences existing in data of different individuals. A case-specific simplified model like this, though not including the full biochemical details of the process, could be used for comparison of different cases of clinical interest.

Materials and methods

The aim of the study is to propose a set of equations that describe the thrombin generation in blood using the minimum possible number of parameters but which are able to describe with acceptable accuracy the whole process. The model is validated against experimental results for thrombin generation in vitro from Thrombin Generation Assays (TGA). The proposed model for thrombin production is based on the cell-based models of coagulation[Smith 2009]; the full description of the biochemical processes are mainly based on [Hoffman and Monroe 2001]. For a detailed modelling of coagulation the localization of the different reactions makes the task more complicated, as it requires taking into account additional parameters such as the binding rate of the substances on cell membranes and the expression, concentration and availability of appropriate binding sites on the cell surfaces. For the development of a simplified model however, it can function as an advantage, as the processes can be grouped in respect to the location they occur (on platelet surface, on the vessel wall or in plasma). This approach is rigorous in cases where the transport of reactants is mainly due to convection such as arterial flow conditions, or in cases where the different species are well mixed. The generation of thrombin and generally the coagulation process is mainly attributed to activated platelets, while the initiation phase is localized on the reacting site of the vessel surface. The burst of thrombin generation is considered to occur when the small amounts of

thrombin produced during the initiation phase cause thrombin concentration to exceed a threshold value. The threshold values used are within the range of thrombin concentration values that have been reported in [Rosing, van Rijn et al. 1985] as being capable of causing platelet activation, 0.5 to 1.2nM of thrombin (0.05 to 0.12U/ml) . The equations of the model are shown in Table 1. The initial values for the reaction rate constants, shown in Table 2, are taken either from already existing models or from experimental studies.

As the proposed model used a reduced number of 4 reactions, each reaction rate represents the integral effect of more than one actual process. Also, ‘activated platelets’ actually represent platelet activity, in the sense that 100% activated platelets implies maximum platelet activity rather than the fact that all platelets are activated. Figure 1a illustrates the actual biochemical reactions that influence each constant while Figure 1b the reduced model. The model is structured as follows: During the initiation phase thrombin generation is described by a slow first order reaction. This reaction, which is localized on the TF-bearing cells, is used to describe the whole pro-coagulant activity that occurs on the TF-bearing cells – formation of the TF-VIIa complex, activation of factors IX, X and V. In this reaction is also included the inhibition of the amounts of IXa, Xa that leave the cell surfaces by TFPI in plasma. The initial value for the reaction rate constant was estimated using the lag times reported in [Lawson, Kalafatis et al. 1994; van't Veer and Mann 1997]. Inhibition of thrombin during this phase is also modelled as a first-order reaction, with the value of the reaction rate constant for thrombin inhibition calculated from the IIa · ATIII inhibition reaction, using the initial bulk concentration of ATIII ($k_{in} = k_{in,ATIII} \cdot \varphi_{ATIII,0} = 1.71 \cdot 10^{-2} s^{-1}$), as this reaction is the major process of thrombin inhibition .(Thrombin inactivation is 77% by anti-thrombin, 14% a₂ macroglobulin and 9% by minor inhibitors [Hemker and Béguin 1995]). With this setup for the initiation phase, the model describes the threshold behaviour of the initiation of blood coagulation in respect to TF concentration[Okorie, Denney et al. 2008;

Shen, Kastrup et al. 2008], as there is a minimum value of activation constant capable of causing thrombin burst and, as this constant is related to the TF concentration (see discussion), a threshold value for TF concentration.

Beyond the point that thrombin concentration has reached the threshold value, the conversion of prothrombin to thrombin is mainly attributed to platelets after their activation. This process is modelled as a second-order reaction, with the initial values for the reaction rate constant used from [Rosing, van Rijn et al. 1985; Sorensen, Burgreen et al. 1999]. Platelets can be activated either by thrombin, if its concentration is greater than the threshold value, or directly by other activated platelets. Thrombin in concentration about 1nM can initiate the activation of platelets [Liu, Freedman et al. 1994], from 0.5nM for minimum activity to 1.2nM for maximal [Rosing, van Rijn et al. 1985]. Platelet activation by thrombin is modelled as a first-order reaction that is initiated when thrombin concentration reaches the threshold value. The activation of platelets by activated platelets represents the activation by platelet-released substances and is modelled as a second order reaction. the reaction rate constants for the activation of platelets used were found in [Kuharsky and Fogelson 2001]. In the case of TF induced coagulation the contribution of the later reaction is negligible, but it can make the model capable of being used to describe shear induced coagulation.

Inhibition of thrombin during the propagation phase is again modelled as a first-order reaction. The reaction rate constant for the inhibition of thrombin in plasma is not the same as for the initiation phase; here we must note that this constant is significantly smaller than the one used in [Leiderman and Fogelson 2011] for modelling this reaction in the same manner, which was based on thrombin half-life in plasma. However, as the activation of protein C that acts as an inhibitor to the coagulation process mainly occurs on the endothelium cells, for the

areas near the endothelium cells the value used for thrombin inhibition is larger, with the exact value derived from the adjustment of the model with the use of TGA results. As demonstrated in Figure 2, the model using the initial parameter values gives reasonable results. By adjusting the values of the constants and parameters of the model within physiological limits, the model can reproduce, to a good level of accuracy, actual thrombin production, by considering the four main parameters of a thrombin generation assay: lag-time (Tlag), maximum concentration (Cmax), time until thrombin concentration reaches the maximum (Tmax) and the estimated thrombin potential (ETP); the last one is represented by the surface under the curve in a thrombin concentration vs time graph. The initial attempts of adjustments were performed manually, but in general the adjustment can be done using the following procedure and assumptions.

Platelet response is very fast compared to the other processes included in the model [Frojmovic, Mooney et al. 1994; Frojmovic, Mooney et al. 1994]. With the approximation that all platelets are activated as soon as thrombin concentration reaches the threshold value, the system of the equations can be analytically solved, giving the equation that describes thrombin concentration through time. This equation has the general form (see appendix 1a):

$$[IIa](t) = \frac{B_i}{A_i - C_i} (e^{A_i t} - e^{C_i t}) = F(t)$$

The equation is similar to the equation proposed in [Wagenvoort, Hemker et al. 2006] but in a non-uniform platelet distribution the results will vary in space. Here the constants A, B and C depend both on the model parameters and TAG results, and they have different values for the initial phase and the propagation phase.

Using the parameters of the TGA and this function we obtain the equations

$$F(Tlag) = [IIa]_{thr}$$

$$F(Tmax) = Cmax$$

$$\frac{dF}{dt}(Tmax) = 0$$

$$\int_0^{\infty} F(t)dt \cong \int_{Tlag}^{t\infty} F(t)dt = ETP$$

221 From this set of equations the constants of the model can be approximated numerically,
 222 making the resulting model equations able to reproduce with the curve of a TGA with given
 223 parameters. In most of the following results only the constants related to thrombin production
 224 $k_{II}^{AP}, k_{surf}, k_{in}$ (see Table 1) were adjusted. In case data from the whole curve is available,
 225 the constants can be approximated as described in appendix 1b.

226 **Results**

227 We first applied the model using the initial values for the constants; while the resulting curve
 228 has the shape of a typical thrombin generation curve, the actual values were significantly
 229 higher than the typical results of TGA for fresh platelet rich plasma as reported in
 230 [Gerotziafas, Depasse et al. 2005]. Performing simulations for different time steps, we found
 231 that the results of the model are identical for time steps below 0.5s (Figure 2). As a whole
 232 heart cycle at rest conditions is about 0.8s (for 75 bpm), the maximum magnitude of the time
 233 steps for simulating pulsating flow is much smaller, thus in terms of temporal discretization,
 234 the coupling of the model with CFD simulations can be straightforward.

235 Subsequently we applied the model in 8 different cases, denoted as Case1-8. In the plots,
 236 when both model and experimental results are represented, model results are named ‘C#
 237 model’ and the experimental results ‘C# exp’. The equations for the adjustment of the
 238 constants were solved in MATLAB, while the adjustment of the platelet related constants was
 239 done manually using Excel and Systems Biology Toolbox 2 [2006]. Case 1 represents the

tuning of the model constants in order to reproduce typical TGA results as reported in [Gerotziafas, Depasse et al. 2005] and the resulting curve (C1 model) is shown in Figure 3 and Figure 4, compared with curves representing slower thrombin generation. In the absence of inhibition (case 2 and case 3), the time interval between the end of the initiation phase and the moment that thrombin concentration reaches its maximum value is 2-4 min, depending on the constant for thrombin activation by activated platelets, and the results match approximately the experimental thrombin production curves found in [Lawson, Kalafatis et al. 1994] (Figure 5).

The next test (Case 4) involved adjusting the model constants in order to fit an arbitrary thrombin generation curve. The experimental curve was found in [Hemker, Giesen et al. 2003]. Figure 6, shows that the model predicts the experimental curve with good accuracy. For future application of the model under flow conditions characterised by non-uniform concentrations of platelets, it has been considered important to test its behaviour with given constants for varying concentration of platelets near to the physiological values. We adjusted the constants so that the model approximated the TGA results for platelet concentration 150×10^9 pl/L (physiological values are $200-400 \times 10^9$ pl/L) and then applied the model with the same setup for two other values of platelet concentrations; Cases 5-7 use the same values for reaction rate constants with platelet concentration 400, 150 and 100×10^9 pl/L respectively. The results shown on Table 3 are within the range of values reported in [Gerotziafas, Depasse et al. 2005] although the dependence of maximum concentration of thrombin on platelet concentration seems a little stronger than for the in vitro experiments. The resulting curves are shown in Figure 3. Further increase of platelet concentration resulted in higher values for maximum thrombin concentration and small decrease of T_{max} , without significant effect on ETP. If the constants describing platelet activation are also suitably modified, the equations can match curves that depict slower thrombin formation like the ones reported in [Allen,

Wolberg et al. 2004] for lower platelet concentrations (75×10^9 pl/L) as shown in Figure 4. The values of the model constants after modification, in order to fit different cases, are shown in Table 4 and for all cases the values are within a reasonable range.

Discussion

This work presents a phenomenological model for thrombin generation that is flexible enough to reproduce a wide range of cases and simple enough to be used for modelling thrombin generation in large scale CFD simulations – in contrast with the most recently suggested models. The four equations of the model are based on the principle assumption that all reactions occur either on the platelet surface or on the reacting site of the vessel wall.

The reactions related to platelet activation actually represent the transition from the initiation to the propagation phase. As the curves used to reproduce a wide range of TGA results correspond to different experiments, these constants vary significantly between two groups of Cases. In the experiments for Cases 1-4, where phospholipids have been used as a substrate for enzymatic reactions, this transition is much faster than for Cases 5-8 where human platelets have been used. For Cases 5-8 the values of these constants have been adjusted manually. It is interesting that the calculated time until platelets reach half of the maximum activity for Case 8 is 5-10 min, in agreement with [Allen, Wolberg et al. 2004]. However, as reported recently [Ninivaggi, Apitz-Castro et al. 2012], TGA results in whole blood resemble the curves of Case 1 and 4, (possibly because red blood cells that are not included in most TGA also contribute to thrombin generation [Ninivaggi, Apitz-Castro et al. 2012; Whelihan and Mann 2013]) so this modification of the parameters related to platelet activation is not necessary for physiological cases and the model can be calibrated as described above. On the other hand with the use of this modification the model could also approximate pathological cases as haemophilia or thrombin generation after anticoagulation treatment. In contrast to

289 the methods described and reviewed in [Brummel-Ziedins 2013] where the effect of the
 290 variation of each factor concentration and activity is investigated, this model uses only the
 291 information included in the TGA curve, thus it has some limitations. For a given value of
 292 inhibition reaction rate, has a maximum lag time that it can reproduce if the reported lag time
 293 is greater than this maximum value, modification of the inhibition constant is required.
 294 Curves corresponding to pathological situations as severe haemophilia A [Wagenvoord,
 295 Hemker et al. 2006]) can be approximated. As factor VIII is mainly involved in the
 296 propagation phase, it is expected that in order to reproduce curves for different fVIII
 297 concentrations the related constants (k_{in} , k_{AP}^{IIa} and k_{IIa}^{AP}) should be modified. As shown in
 298 Figure 8, this can be done (the concentrations of VIII have been calculated using 12.8 hours
 299 as half-life of fVIII [van Dijk, van der Bom et al. 2005]). At first sight, the most significant
 300 inaccuracy of the model (when the initial values of the parameters are used) is that the time
 301 interval between the initiation of thrombin burst and maximum concentration of thrombin is
 302 smaller than the one reported in TGAs (2.8min compared to 2min predicted by the model)
 303 when adjusting only the three previously mentioned parameters. The increase of thrombin
 304 concentration predicted by the model is sharper compared to the experimental data and the
 305 shapes of the two curves differ for this time interval. That can be fixed by adjusting manually
 306 the constants related to platelet activation as we did for Cases 4-8. However the experimental
 307 data, while in all studies presented in the form of curves, in some cases actually correspond to
 308 measurements in discrete time intervals and the resulting curves are obtained through data
 309 fitting. In Figure 7 a plot of three curves is shown, for the time interval of thrombin
 310 concentration increase, obtained from the same model results. In one case (dense) the time
 311 interval between two data points is 2s, while for the other two cases (sparse1 and sparse2) is
 312 30s and 20s respectively –reasonable time intervals between the withdrawal of two samples.
 313 It is obvious that curve fitting on experimental values, used in studies prior to the introduction

of continuous monitoring of thrombin generation, while making the results more presentable can also give incorrect information on the actual evolution of the process between two measurements, so differences between modelled and experimental curves do not necessary indicate inadequacy of the model.

The constant that represents the initial thrombin production rate k_{surf} (for a given value of the inhibition rate) is mainly determined by the lag time. While there is dependence of different experiments' results on the exact composition of the samples and the triggering substance used, for the case described in [van't Veer and Mann 1997; Gerotziafas, Depasse et al. 2005], there seems to be a clear relationship ($R^2=0.989$) between TF concentration and k_{surf} for the same experimental conditions and TF concentrations between 1 and 30pM:

$$k_{surf} = k_{surf,max}(A + B \ln \left(\frac{[TF]}{[TF_{max}]} \right))$$

The constant values are $A = 0.996 \approx 1$, $B = 0.0372$ while for the aforementioned study the maximum calculated value for the rate of thrombin generation during the initiation phase is $k_{surf,max} = 7.91 \cdot 10^{-6} s^{-1}$ and the relationship can approximately be written as:

$$k_{surf} = k_{surf,max}(1 + 0.0372 \cdot \ln \left(\frac{[TF]}{[TF_{max}]} \right))$$

These relationship gives good result when estimating k_{surf} in other studies with similar methodology, but for studies using recombinant TF:VIIa as trigger for the coagulation process, while the a good correlation between k_{surf} and trigger concentration can be established, ($R^2>0.98$) the resulting formulas are different.

For the case of thrombus formation on a reacting site of a blood vessel wall, the term representing the slow phase of thrombin generation corresponds to a surface reaction term.

The reaction rate for the surface reaction can be calculated with the use of the reported surface TF concentration in atheromatous plaques (33pg/cm²) [Bonderman, Teml et al. 2002] and the molecular weight of (46,000Da approximately [Arabinda Guha 1986]). For a computational cubic cell of e.g. 100µm this numbers would lead to a TF concentration of about 70pM resulting to $k_{surf} = 9.75 \cdot 10^{-6} s^{-1}$. Sub-threshold concentration of thrombin actually represents also the products of the previous steps of coagulation. At the same time this approach allows a slow rate of fibrin production before the burst of thrombin and a realistic prediction of clotting time. As TGA results demonstrate inter-laboratory variation [Van Veen, Gatt et al. 2008], this model, based on TGA results and with its simplified character, does not claim to reproduce with precise accuracy thrombin generation but offers a way to model thrombin generation that (1) has comparative value, in the sense that it can be adjusted to describe different rates of thrombin generation, and (2) can be easily coupled with CFD simulations. We believe that these equations, if combined with two more, one describing fibrin formation and one describing platelet deposition on the reacting site of the vessel, can be used as a thrombus formation model for three dimensional CFD simulations in blood vessels. The results of such a model can be used to compare the evolution of thrombus formation in different cases and for different thrombogenic potential of human blood. Finally, as the model describes the production of thrombin in blood in a phenomenological way, it does not require additional information regarding the concentration of different factors and the details for every reaction in the coagulation system and it can be calibrated and applied directly for different cases based only on the parameters or the curve of the TGA (or the curve itself).

Declarations

Competing interests: None declared

357 Funding: None

358 Ethical approval: Not required

359

360 (4,585 words)

361 **References**

- 362 Allen, G., A. Wolberg, et al. (2004). "Impact of procoagulant concentration on rate, peak and
363 total thrombin generation in a model system." Journal of Thrombosis and
364 Haemostasis **2**(3): 402-413.
- 365 Anand, M., K. Rajagopal, et al. (2003). "A Model Incorporating some of the Mechanical and
366 Biochemical Factors Underlying Clot Formation and Dissolution in Flowing Blood."
367 Journal of Theoretical Medicine **5**(3-4): 183-218.
- 368 Anand, M., K. Rajagopal, et al. (2005). "A Model for the Formation and Lysis of Blood
369 Clots." Pathophysiology of Haemostasis and Thrombosis **34**(2-3): 109-120.
- 370 Arabinda Guha, R. B., William Konigsberg and Yale Nemerson (1986). "Affinity purification
371 of human tissue factor: Interaction of factor VII and tissue factor in detergent
372 micelles." Biochemistry **83**: 299-302.
- 373 Badimon, L., J. J. Badimon, et al. (1986). "Influence of arterial damage and wall shear rate on
374 platelet deposition. Ex vivo study in a swine model." Arteriosclerosis, Thrombosis,
375 and Vascular Biology **6**(3): 312-320.
- 376 Beltrami, E. and J. Jesty (1995). "Mathematical analysis of activation thresholds in enzyme-
377 catalyzed positive feedbacks: application to the feedbacks of blood coagulation."
378 Proceedings of the National academy of Sciences of the United States of America
379 **92**(19): 8744-8748.
- 380 Bodnár, T. and A. Sequeira (2008). "Numerical simulation of the coagulation dynamics of
381 blood." Computational and Mathematical Methods in Medicine **9**(2): 83-104.
- 382 Bonderman, D., A. Teml, et al. (2002). "Coronary no-reflow is caused by shedding of active
383 tissue factor from dissected atherosclerotic plaque." Blood **99**(8): 2794-2800.
- 384 Brass, L. F. (2003). "Thrombin and Platelet Activation*." CHEST Journal **124**(3_suppl):
385 18S-25S.
- 386 Brummel-Ziedins, K. (2013). "Models for thrombin generation and risk of disease." Journal
387 of Thrombosis and Haemostasis **11**: 212-223.
- 388 Fernández-Ortiz, A., J. J. Badimon, et al. (1994). "Characterization of the relative
389 thrombogenicity of atherosclerotic plaque components: Implications for consequences
390 of plaque rupture." Journal of the American College of Cardiology **23**(7): 1562-1569.
- 391 Fogelson, A. L. and R. D. Guy (2004). "Platelet-wall interactions in continuum models of
392 platelet thrombosis: formulation and numerical solution." Mathematical Medicine and
393 Biology **21**(4): 293-334.
- 394 Fogelson, A. L. and R. D. Guy (2008). "Immersed-boundary-type models of intravascular
395 platelet aggregation." Computer Methods in Applied Mechanics and Engineering
396 **197**(25-28): 2087-2104.
- 397 Fogelson, A. L. and N. Tania (2005). "Coagulation under Flow: The Influence of Flow-
398 Mediated Transport on the Initiation and Inhibition of Coagulation." Pathophysiology

- of Haemostasis and Thrombosis **34**(2-3): 91-108.
- Folie, B. J. and L. V. McIntire (1989). "Mathematical analysis of mural thrombogenesis. Concentration profiles of platelet-activating agents and effects of viscous shear flow." Biophysical Journal **56**(6): 1121-1141.
- Frojmovic, M. M., R. F. Mooney, et al. (1994). "Dynamics of platelet glycoprotein IIb-IIIa receptor expression and fibrinogen binding. I. Quantal activation of platelet subpopulations varies with adenosine diphosphate concentration." Biophysical Journal **67**(5): 2060-2068.
- Frojmovic, M. M., R. F. Mooney, et al. (1994). "Dynamics of platelet glycoprotein IIb-IIIa receptor expression and fibrinogen binding. II. Quantal activation parallels platelet capture in stir-associated microaggregation." Biophysical Journal **67**(5): 2069-2075.
- Furie, B. and B. C. Furie (2008). "Mechanisms of Thrombus Formation." New England Journal of Medicine **359**(9): 938-949.
- Gerotziafas, G. T., F. Depasse, et al. (2005). "Towards a standardization of thrombin generation assessment: The influence of tissue factor, platelets and phospholipids concentration on the normal values of Thrombogram-TrombinoScope assay." Thrombosis Journal **3**(16).
- Gibson, C. M., L. Diaz, et al. (1993). "Relation of vessel wall shear stress to atherosclerosis progression in human coronary arteries." Arteriosclerosis, Thrombosis, and Vascular Biology **13**(2): 310-315.
- Hemker, H. C. and S. Béguin (1995). "Thrombin generation in plasma: its assessment via the endogenous thrombin potential." Thrombosis and haemostasis **74**(1): 134-138.
- Hemker, H. C., P. Giesen, et al. (2003). "Calibrated automated thrombin generation measurement in clotting plasma." Pathophysiology of Haemostasis and Thrombosis **33**(1): 4-15.
- Hockin, M. F., K. C. Jones, et al. (2002). "A Model for the Stoichiometric Regulation of Blood Coagulation." Journal of Biological Chemistry **277**(21): 18322-18333.
- Hoffman, M. and D. M. Monroe (2001). "A cell-based model of hemostasis." Thrombosis and haemostasis **85**(6): 958-965.
- Hubbell, J. A. and L. V. McIntire (1986). "Platelet active concentration profiles near growing thrombi. A mathematical consideration." Biophysical Journal **50**(5): 937-945.
- Jesty, J., W. Yin, et al. (2003). "Platelet activation in a circulating flow loop: combined effects of shear stress and exposure time." Platelets **14**(3): 143-149.
- Jones, K. C. and K. G. Mann (1994). "A model for the tissue factor pathway to thrombin. II. A mathematical simulation." Journal of Biological Chemistry **269**(37): 23367-23373.
- Kuharsky, A. L. and A. L. Fogelson (2001). "Surface-Mediated Control of Blood Coagulation: The Role of Binding Site Densities and Platelet Deposition." Biophysical Journal **80**(3): 1050-1074.
- Lai, M.-C. and C. S. Peskin (2000). "An Immersed Boundary Method with Formal Second-Order Accuracy and Reduced Numerical Viscosity." Journal of Computational Physics **160**(2): 705-719.
- Lawson, J. H., M. Kalafatis, et al. (1994). "A model for the tissue factor pathway to thrombin. I. An empirical study." Journal of Biological Chemistry **269**(37): 23357-23366.
- Leiderman, K. and A. L. Fogelson (2011). "Grow with the flow: a spatial-temporal model of platelet deposition and blood coagulation under flow." Mathematical Medicine and Biology **28**(1): 47-84.
- Liu, L., J. Freedman, et al. (1994). "Thrombin binding to platelets and their activation in plasma." British Journal of Haematology **88**(3): 592-600.
- Lo, K., W. S. Denney, et al. (2005). "Stochastic Modeling of Blood Coagulation Initiation." Pathophysiology of Haemostasis and Thrombosis **34**(2-3): 80-90.

- Marée, A. M., V. Grieneisen, et al. (2007). The Cellular Potts Model and Biophysical Properties of Cells, Tissues and Morphogenesis. Single-Cell-Based Models in Biology and Medicine. A. A. Anderson, M. J. Chaplain and K. Rejniak, Birkhäuser Basel: 107-136.
- Monroe, D. M., M. Hoffman, et al. (2002). "Platelets and Thrombin Generation." Arteriosclerosis, Thrombosis, and Vascular Biology **22**(9): 1381-1389.
- Mosesson, M. W. (2005). "Fibrinogen and fibrin structure and functions." Journal of Thrombosis and Haemostasis **3**(8): 1894-1904.
- Nesbitt, W. S., E. Westein, et al. (2009). "A shear gradient-dependent platelet aggregation mechanism drives thrombus formation." Nat Med **15**(6): 665-673.
- Ninivaggi, M., R. Apitz-Castro, et al. (2012). "Whole-Blood Thrombin Generation Monitored with a Calibrated Automated Thrombogram-Based Assay." Clinical Chemistry **58**(8): 1252-1259.
- Okorie, U. M., W. S. Denney, et al. (2008). "Determination of surface tissue factor thresholds that trigger coagulation at venous and arterial shear rates: amplification of 100 fM circulating tissue factor requires flow." Blood **111**(7): 3507-3513.
- Oliver, J. A., D. M. Monroe, et al. (1999). "Thrombin Activates Factor XI on Activated Platelets in the Absence of Factor XII." Arteriosclerosis, Thrombosis, and Vascular Biology **19**(1): 170-177.
- Peskin, C. S. (2002). "The immersed boundary method." Acta Numerica **11**: 479-517.
- Qiao, Y. H., C. Q. Xu, et al. (2004). "The kinetic model and simulation of blood coagulation-the kinetic influence of activated protein C." Medical Engineering & Physics **26**(4): 341-347.
- Rauch, U., J. I. Osende, et al. (2001). "Thrombus formation on atherosclerotic plaques: pathogenesis and clinical consequences." Annals of internal medicine **134**(3): 224-238.
- Reininger, A. J., I. Bernlochner, et al. (2010). "A 2-Step Mechanism of Arterial Thrombus Formation Induced by Human Atherosclerotic Plaques." Journal of the American College of Cardiology **55**(11): 1147-1158.
- Rendu, F. and B. Brohard-Bohn (2001). "The platelet release reaction: granules' constituents, secretion and functions." Platelets **12**(5): 261-273.
- Rosing, J., J. van Rijn, et al. (1985). "The role of activated human platelets in prothrombin and factor X activation." Blood **65**(2): 319-332.
- SBtoolbox (2006). "Systems Biology Toolbox for MATLAB: A computational platform for research in Systems Biology." Bioinformatics and Biology Insights **22**(4): 514-515.
- Shen, F., C. J. Kastrup, et al. (2008). "Threshold Response of Initiation of Blood Coagulation by Tissue Factor in Patterned Microfluidic Capillaries Is Controlled by Shear Rate." Arteriosclerosis, Thrombosis, and Vascular Biology **28**(11): 2035-2041.
- Smith, S. A. (2009). "The cell-based model of coagulation." Journal of Veterinary Emergency and Critical Care **19**(1): 3-10.
- Sorensen, E. N., G. W. Burgreen, et al. (1999). "Computational Simulation of Platelet Deposition and Activation: I. Model Development and Properties." Annals of Biomedical Engineering **27**(4): 436-448.
- van't Veer, C. and K. G. Mann (1997). "Regulation of Tissue Factor Initiated Thrombin Generation by the Stoichiometric Inhibitors Tissue Factor Pathway Inhibitor, Antithrombin-III, and Heparin Cofactor-II." Journal of Biological Chemistry **272**(7): 4367-4377.
- van Dijk, K., J. G. van der Bom, et al. (2005). "Factor VIII half-life and clinical phenotype of severe hemophilia A." Haematologica **90**(4): 494-498.
- Van Veen, J., A. Gatt, et al. (2008). "Thrombin generation testing in routine clinical practice:

- are we there yet?" British Journal of Haematology **142**(6): 889-903.
- Wagenvoord, R., P. W. Hemker, et al. (2006). "The limits of simulation of the clotting system." Journal of Thrombosis and Haemostasis **4**(6): 1331-1338.
- Whelihan, M. F. and K. G. Mann (2013). "The role of the red cell membrane in thrombin generation." Thrombosis Research.
- Willems, G., T. Lindhout, et al. (1991). "Simulation Model for Thrombin Generation in Plasma." Pathophysiology of Haemostasis and Thrombosis **21**(4): 197-207.
- Xu, C., X. Hu Xu, et al. (2005). "Simulation of a mathematical model of the role of the TFPI in the extrinsic pathway of coagulation." Computers in Biology and Medicine **35**(5): 435-445.
- Xu, Z., N. Chen, et al. (2008). "A multiscale model of thrombus development." Journal of The Royal Society Interface **5**(24): 705-722.
- Xu, Z., N. Chen, et al. (2009). "Study of blood flow impact on growth of thrombi using a multiscale model." Soft Matter **5**(4): 769-779.
- Xu, Z., J. Lioi, et al. (2010). "A Multiscale Model of Venous Thrombus Formation with Surface-Mediated Control of Blood Coagulation Cascade." Biophysical Journal **98**(9): 1723-1732.
- Yang, X. S., R. W. Lewis, et al. (2004). "Finite Element Analysis of Fogelson's Model for Platelet Aggregation."
- Zarnitsina, V. I., A. V. Pokhilko, et al. (1996). "A Mathematical model for the spatio-temporal dynamics of intrinsic pathway of blood coagulation. I. The model description." Thrombosis Research **84**(4): 225-236.
- Zarnitsina, V. I., A. V. Pokhilko, et al. (1996). "A Mathematical model for the spatio-temporal dynamics of intrinsic pathway of blood coagulation. II. Results." Thrombosis Research **84**(5): 333-344.

Appendix: Equations' solution:

- a. Under the assumption that all platelets are instantly activated when thrombin reaches its threshold value, the concentration of platelets is zero when thrombin concentration is below the threshold value and equal to the resting platelet concentration when thrombin exceeds the threshold values. The equations describing thrombin and prothrombin concentration become:

$\frac{\partial [IIa]}{\partial t} = -k_{in}[IIa] + k_{tot} \cdot [II]$
$\frac{\partial [II]}{\partial t} = -k_{tot} \cdot [II]$

Here k_{tot} represent the total rate of prothrombin conversion to thrombin and includes both the production on the reacting site and on the platelet surfaces:

$$k_{tot} = k_{surf} + k_{II}^{AP} \cdot [PL], \text{ if } [IIa] > [IIa]_{th}$$

$$k_{tot} = k_{surf}, \quad \text{if } [IIa] \leq [IIa]_{th}$$

533 This leads to a direct solution for prothrombin concentration:

$$[II](t) = [II](t = 0) \cdot e^{-k_{tot} \cdot t}$$

534 The D.E. describing thrombin concentration becomes:

$$\frac{\partial [IIa]}{\partial t} = -k_{in}[IIa] + k_{tot} \cdot [II]_o \cdot e^{-k_{tot} \cdot t}, \text{ or } \frac{dx}{dt} = Ax - CB e^{Ct}$$

$$\text{where } A = -k_{in}, B = [II]_o \text{ and } C = -k_{tot}$$

535 The equation can be rewritten as follows,

$$\frac{dy}{dt} = (A - C) \cdot y - CB, \text{ where } y = x \cdot e^{-Ct}$$

536 The last expression, after manipulation leads to an (approximate because of the aforementioned

537 assumption) analytic solution for the temporal evolution of thrombin concentration (X):

$$X(t) = \frac{e^{Ct}}{A - C} [(A - C)X_0 e^{-Ct_0} - CB] e^{(A-C)t} + CB \text{ or}$$

$$[IIa](t) = \frac{e^{-k_{tot} \cdot t}}{k_{tot} - k_{in}} [(k_{tot} - k_{in})[IIa]_0 e^{k_{tot} \cdot t_0} + k_{tot} \cdot [II]_o] e^{(k_{tot} - k_{in}) \cdot t} - k_{tot} \cdot [II]_o$$

538

539 For $[IIa](t = 0) = 0$ the equation gets the simplified form:

$$[IIa](t) = \frac{k_{tot} \cdot [II]_o}{k_{in} - k_{tot}} (e^{-k_{tot} \cdot t} - e^{-k_{in} \cdot t})$$

540 b. In the case the data from the whole curve is available, there is another way for

541 obtaining the model constants. The reaction rate is obtained by solving (numerically)

the last equation:

$$[IIa]_{th} - \frac{k_{surf} \cdot [II]_o}{k_{in} - k_{surf}} (e^{-k_{surf} Tlag} - e^{-k_{in} Tlag}) = 0$$

As the activated platelet concentration is approximately,

$$[AP] = [RP](0) \left(1 - e^{-(t-Tlag)k_{AP}^{IIa}}\right), t > Tlag$$

Analytical expression can be obtained for prothrombin concentration versus time,

$$[II](t) = [II](t = 0) \cdot e^{-k_{tot}(t) \cdot t} \text{ and therefore for the differential equation}$$

$$\text{describing thrombin evolution for } t > Tlag, \frac{d}{dt} [IIa] = -k'_{in} \cdot [IIa] + k_{tot}(t) \cdot [II](t)$$

and the constants can be obtained numerically using an iterative process.

List of Figures

Figure 1: Schematic representation of cell based model for blood coagulation (reproduced from Smith et al 2009). (a) and the reduced model (b). The different coloured arrows represent the actual processes that are lumped in each reaction rate constant. Red: Inhibition of thrombin in plasma by ATIII and near the vessel wall by APC. Green: Platelet activation by thrombin. Purple: thrombin production by activated platelets. Yellow: Thrombin production in plasma near the reacting site on vessel wall, includes all the reactions from binding of VIIa on TF up to the generation of small amounts of IIa and also (mostly) the inhibition of all other species except thrombin. Turquase: Activation of platelets by substances released by activated platelets such as ADP.

Figure 2: Results of the model for different time steps. For time steps below 0.5s the results coincide.

Figure 3: Behaviour of the model for different initial platelet concentrations.

Figure 4: Adjustment of the model in order to reproduce slower thrombin generation, experimental data.¹

563 **Figure 5:** Model results for thrombin production without inhibition, adjusted to fit the results
564 reported in²⁷

565 **Figure 6:** Capability of the model to reproduce an arbitrary thrombin generation curve²⁰

566 **Figure 7:** Dependence of the shape of the curve on the time interval between two data
567 points. While the initial results are the same curve fitting on data produces significantly
568 different curves

569 **Figure 8:** Reproduction of thrombin generation curves corresponding to different fVIII
570 concentrations and the normalized modification of the related constants.

571

572 **Tables, figures**

573 Table 1: Equations of the model

Thrombin (IIa)	$\frac{\partial[IIa]}{\partial t} = -k_{in}[IIa] + (k_{surf} + k_{II}^{AP} \cdot [AP]) \cdot [II]$
Prothrombin (II)	$\frac{\partial[II]}{\partial t} = -(k_{surf} + k_{II}^{AP} \cdot [AP]) \cdot [II]$
Activated Platelets (AP)	$\frac{\partial[AP]}{\partial t} = k_{AP}^{AP} \cdot [AP] \cdot [RP] + k_{AP}^{IIa} \cdot [RP]$
Resting Platelets (RP)	$\frac{\partial[RP]}{\partial t} = -k_{AP}^{AP} \cdot [AP] \cdot [RP] - k_{AP}^{IIa} \cdot [RP]$

574

575 Table 2: Constants and parameters

Process	Constant symbol	Initial value (S.I.)	Reference
Thrombin generation by activated platelets	k_{II}^{AP}	$0.0856 - 1.81s^{-1}$	[Rosing, van Rijn et al. 1985; Sorensen, Burgreen et al. 1999]
Thrombin generation on reacting surface	k_{surf}	$10^{-5}s^{-1}$	n/a
Platelet activation by thrombin	k_{AP}^{IIa}	$0, if [IIa] < [IIa]_{thr}$ $0.5, if [IIa] \geq [IIa]_{thr}$	[Kuharsky and Fogelson 2001]
Platelet activation by activated platelets	k_{AP}^{AP}	$5.24 \cdot 10^{-2}s^{-1}$	[Kuharsky and Fogelson 2001]
Thrombin inhibition*	k_{in}	$1.71 \cdot 10^{-2} - 0.2s^{-1}$	[Hockin, Jones et al. 2002; Leiderman and Fogelson 2011]
Thrombin concentration threshold for platelet activation	$[IIa]_{thr}$	$1.75 - 4.18 \cdot 10^{-8}kg/kg$ (0.5-1.2nM or 0.05-0.12U/ml)	[Rosing, van Rijn et al. 1985]

577 Table 3: Results of the model for different cases

		Tlag (min)	Tmax (min)	Cmax (nM)	ETP (nM·min)
Case 1	experiment	3.6 ± 0.8	7.4 ± 1.8	164 ± 50	1321 ± 330
	model	3.7	6.8	165	1364
Case 2	experiment	1.5	3.5	$(1.5 \cdot 10^3)$	n/a
	model	1.5	4	$(1.5 \cdot 10^3)$	n/a
Case 3	experiment	0.67	2.25	$(1.5 \cdot 10^3)$	n/a
	model	0.65	2.38	$(1.5 \cdot 10^3)$	n/a
Case 4	experiment	3.5	4.8	199	735
	model	3.7	4.6	196	710
Case 5	experiment	5 ± 0.5	11 ± 2.7	161 ± 38	1633 ± 81
	model	5.8	9	190	1718
Case 6	experiment	5.5 ± 0.5	11 ± 0.2	98 ± 40	1316 ± 255
	model	6	9.4	91	1370
Case 7	experiment	5.8 ± 0.7	13 ± 0.9	72 ± 38	1135 ± 300
	model	6	9.6	62	1118
Case 8	experiment	15	27	101	2012
	model	13.3	25.3	102	1934

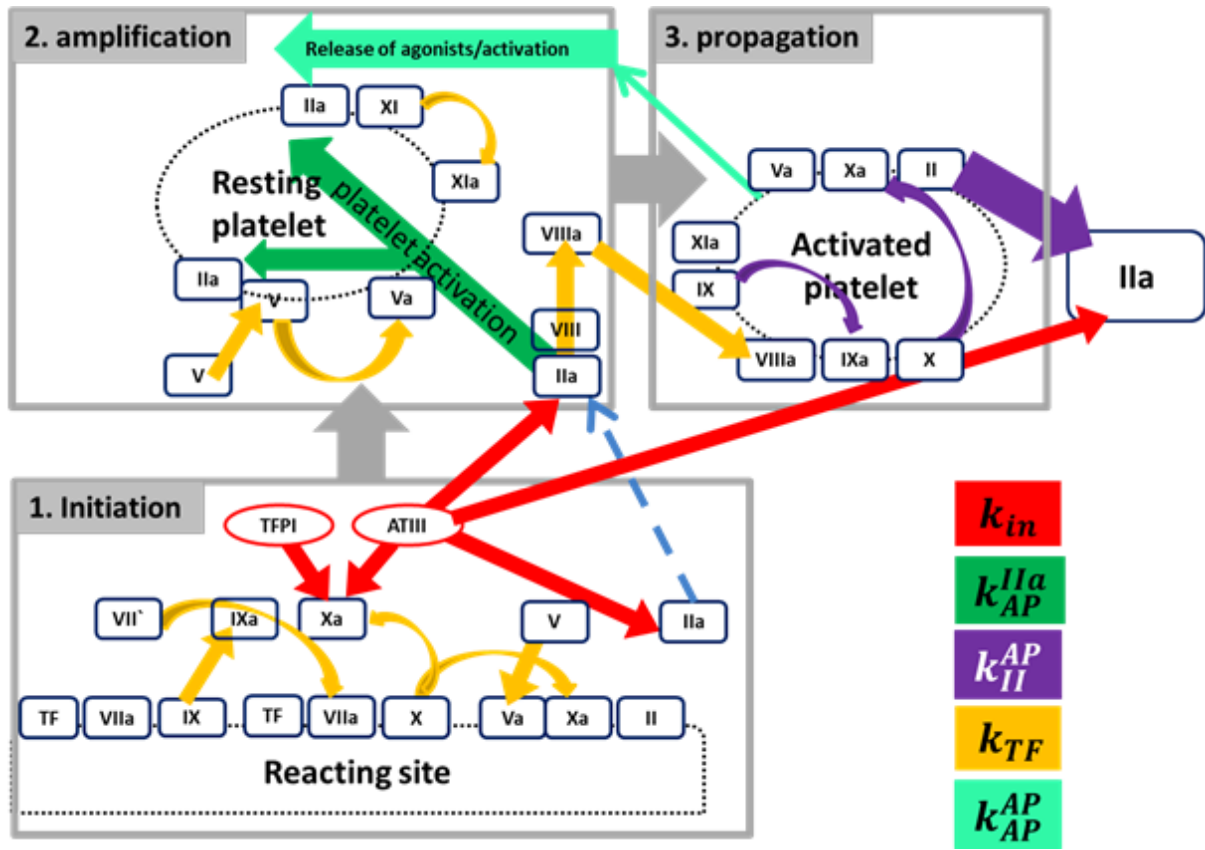
578

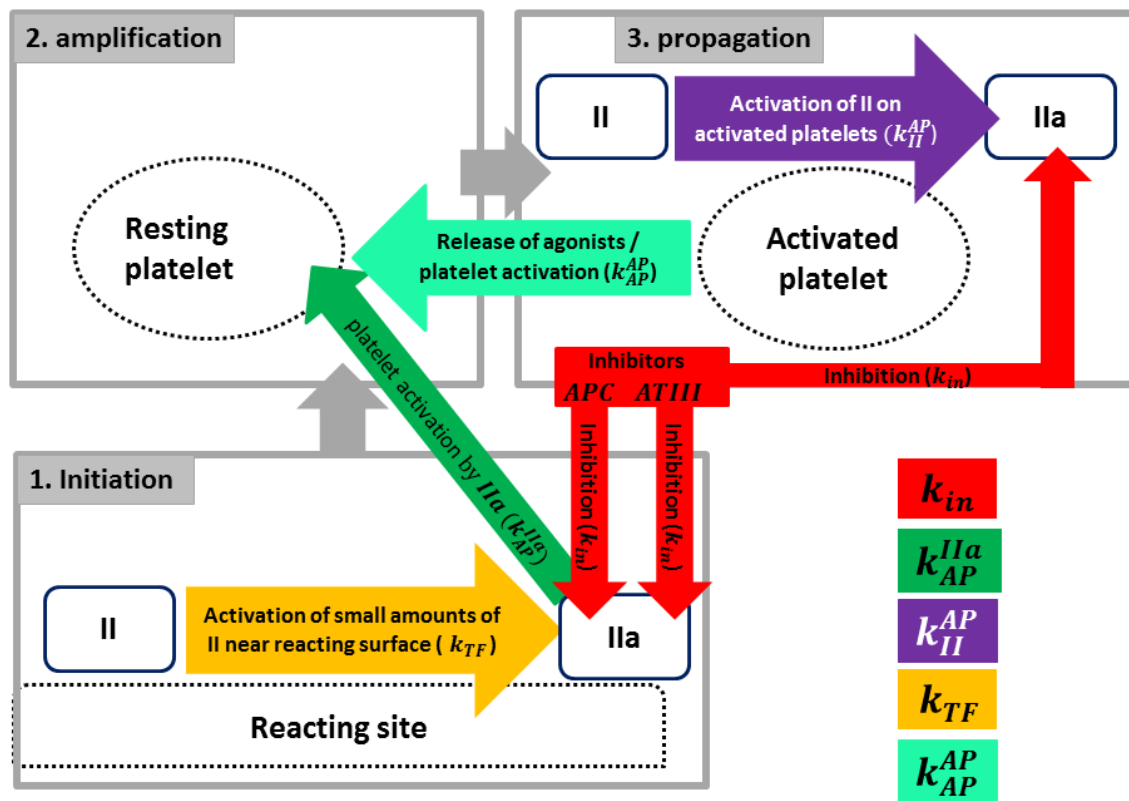
579

Table 4: The variation of the model constants after adjustment in order to reproduce different cases

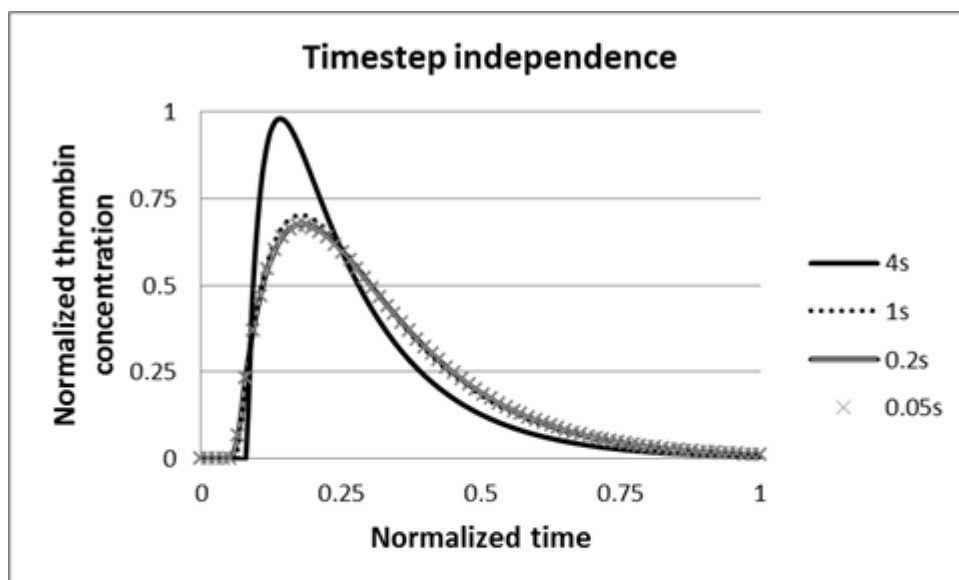
Constant	Initial estimations	Case 1	Case 2	Case 3	Case 4	Cases 5-7	Case 8
$k_{surf}(s^{-1})$	10^{-5}	$7.367 \cdot 10^{-6}$	$9.162 \cdot 10^{-6}$	$1.511 \cdot 10^{-5}$	$7.367 \cdot 10^{-6}$	$7.223 \cdot 10^{-6}$	$4.06 \cdot 10^{-7}$
$k_{II}^{AP}(s^{-1})$	$0.0856 - 1.81$	0.73	2.8	4	1.55	0.525	3.6
$k_{in}(s^{-1})$	$1.71 \cdot 10^{-2}$ $- 0.2$	0.032	0	0	0.052	0.0262	0.024
$k_{AP}^{IIa}(s^{-1})$	$0.2 - 0.5$	-	-	0.5	0.5	0.002	0.0018

Figure 1a

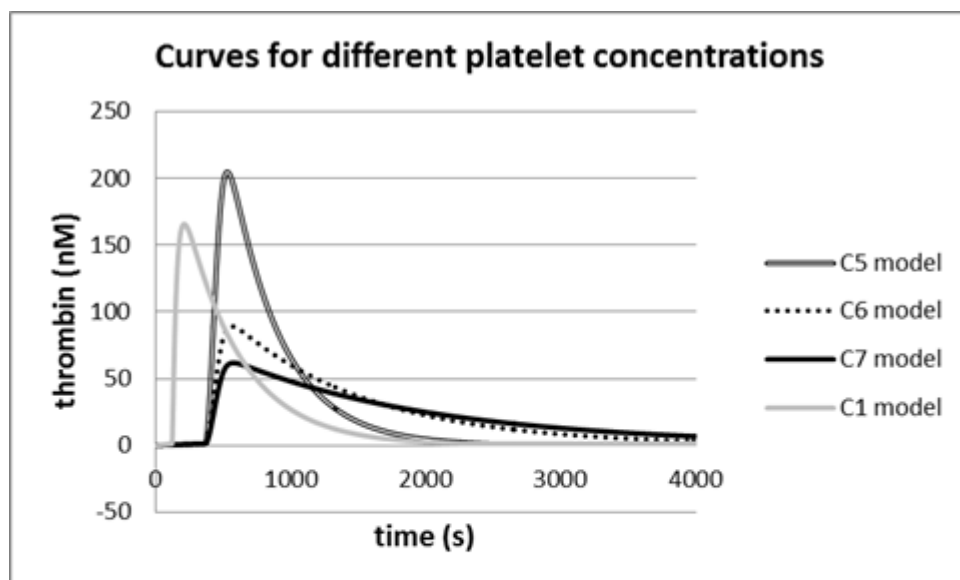


586 **Figure 1b**

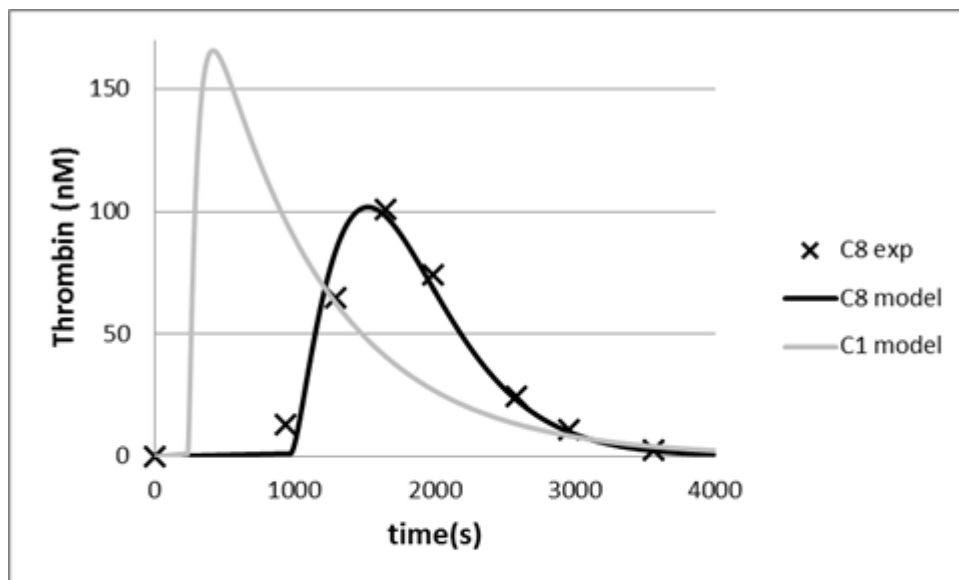
587

588 **Figure 2**

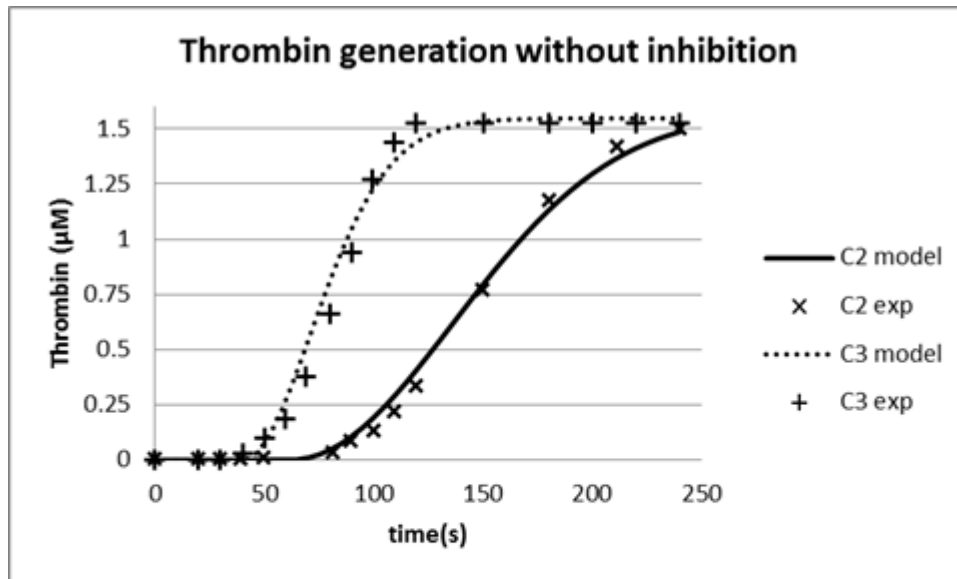
589

590 **Figure 3**

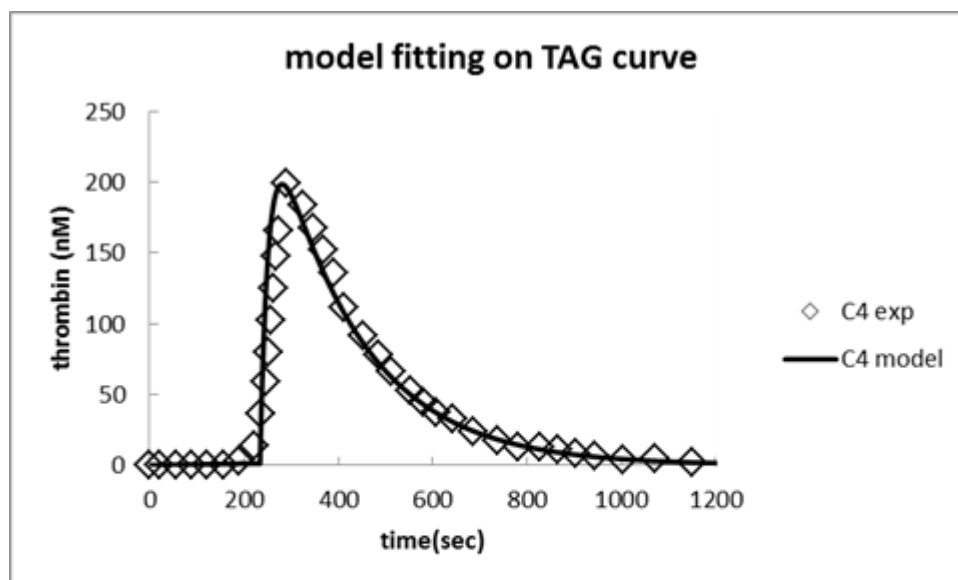
591

592 **Figure 4**

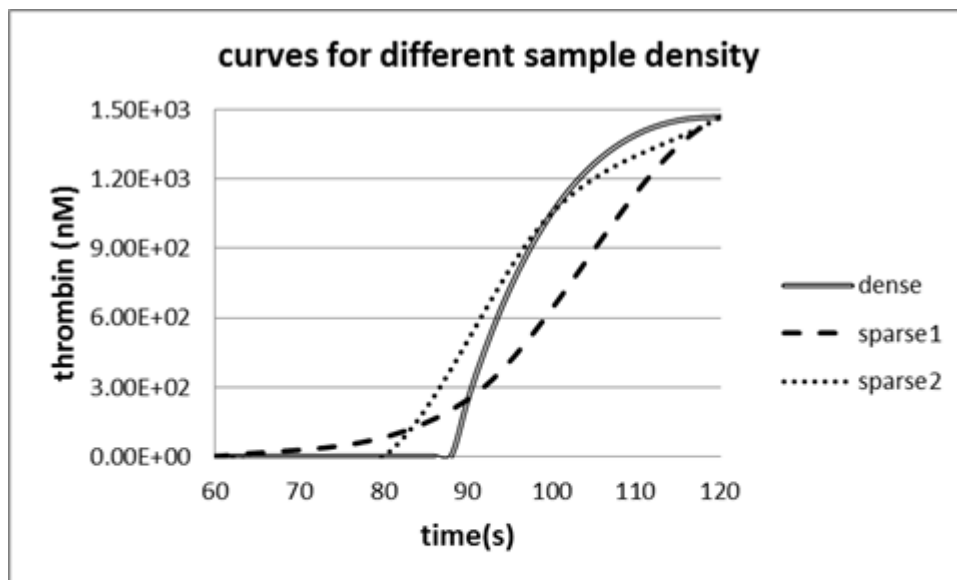
593

594 **Figure 5**

595

596 **Figure 6**

597

598 **Figure 7**

599

Figure 8